

CFD Simulation of Static Thrust Generated by an Airfoil-Based Propeller Using ANSYS Fluent

El Mehdi Adib Alaoui

December 2025

1 Abstract

Small propellers are used in various applications such as small unmanned aerial vehicles and hobby aircraft, as well as test rigs located in low-speed wind tunnels. The applicable thrust serves as one of the crucial operational parameters of such designs, affecting their payload, climb rate, and overall efficiency. In fact, thrust is obtained primarily via stand test with load cell, and it is a laborious task performed individually each time for each new propeller motor combination. For this reason, accurate numerical model is very useful in the design phase, predicting thrust trends with changing rotational speed before hardware is built. Since this moment Computational Fluid Dynamics (CFD) is a common solution. CFD is then used to provide pressure distribution and corresponding aerodynamic forces to the propeller after 3D flow has been resolved around the blades. This process is then, at the same time, influenced by modeling decisions, such as the size of the computational domain, mesh quality, the turbulence model type, and the rotation method that is selected. A straightforward explanation of these choices is essential to ensure performance is reliable or to show the comparison to the possible next work is meaningful or for the next work. We run a 254 mm two-bladed propeller in ANSYS Fluent CFD simulation. This geometry is enclosed in a rectangular unit divided between rotating inner domain around the propeller and surrounding static domain. This mesh is prepared in part by using unstructured tetrahedral elements, with local reinforcement on the propeller, inlet, and outlet surface area. Usually air is an incompressible fluid of constant density and viscosity, and turbulence in turbulent materials is modeled by a two-equation RANS. Upstream, a velocity inlet is established and a pressure outlet downstream is found. A rotational velocity is given to the inner fluid region indicating the rotation of the propeller. The main objective is to calculate the thrust generated by the propeller on a number of rotational speeds and study the rotation of the thrust change along RPM. Once the transient solution is in this periodic form, the force reports on the propeller surface can then be used to extract axial forces. The model is basic leveled, not all the effective effects have to be valid so we have a rough estimation of thrust levels to follow and next the framework is used as a reference point for mesh refinement, advanced turbulence models or experimental data verification so it will be developed to be better.

2 Introduction

In this project we utilize ANSYS Fluent to conduct a three-dimensional transient CFD analysis for a 254 mm propeller, comprised of two blades, as the thrust source. The computational domain is a cylindrical rotating sub-domain surrounding the propeller, enclosed in a rectangular static enclosure. This consists in discretizing the flow in an unstructured tetrahedral mesh (global element size 80 mm, reduced to 40 mm near the propeller and inlet/outlet surfaces), and modeling the air as an incompressible Newtonian fluid with constant density 1.225 kg/m^3 and viscosity $1.7894 \times 10^{-5} \text{ kg/(m} \cdot \text{s)}$. We deploy a velocity inlet with 5% turbulence intensity and $k-\varepsilon$ turbulence closure in a realizable way upstream, and we apply a pressure outlet downstream. From 1400 rpm to 2000 rpm, the speed of the shaft is transiently simulated by prescribing the rotational travel in the inner fluid area. The thrust is determined by integrating the pressure and viscous forces at the propeller surface with a force report definition. While the predicted thrust increased from 4.40 N at 1400 rpm to 6.12 N at 1500 rpm and 10.33 N at 2000 rpm, the high nonlinear dependence of the propulsive behavior against the rotational speed is demonstrated.

3 Theoretical Analysis

The static propulsive efficiency of the propeller is defined as

$$\eta = \frac{T \bar{V}}{P}, \quad (1)$$

where T is the thrust, \bar{V} is the representative flow velocity through the propeller disc and P is the shaft power. In this project an efficiency of $\eta = 85\%$ is assumed for the experimental case.

1D momentum model

For a static case the upstream velocity is taken as $V = 0$. The slipstream velocity downstream of the propeller is denoted by V_s , and the average axial velocity through the disc is approximated by

$$V_0 = \frac{V_s + V}{2}. \quad (2)$$

With $V = 0$ this reduces to

$$V_0 = \frac{V_s}{2}. \quad (3)$$

The mass flow rate through the propeller disc is

$$\dot{m} = \rho S V_0, \quad (4)$$

with ρ the air density and S the disc area. The thrust comes from the axial momentum change:

$$T = \dot{m} (V_s - V). \quad (5)$$

Substituting $V_s = 2V_0$ and $V = 0$ gives

$$T = \dot{m} (2V_0) = \rho S V_0 (2V_0) = 2\rho S V_0^2. \quad (6)$$

The ideal power needed to generate the slipstream is obtained from the kinetic-energy increase of the flow:

$$P = \frac{1}{2} \dot{m} V_s^2 = \frac{1}{2} \rho S V_0 (2V_0)^2 = 2\rho S V_0^3. \quad (7)$$

Thrust as a function of power

From the power expression,

$$P = 2\rho S V_0^3, \quad (8)$$

the induced velocity can be written as

$$V_0 = \left(\frac{P}{2\rho S} \right)^{1/3}. \quad (9)$$

Substituting this into the thrust expression $T = 2\rho S V_0^2$ gives $T_{ideal} = 2\rho S \left(\frac{P}{2\rho S} \right)^{2/3}$

$$= (2\rho S)^{1/3} P^{2/3} = (2\rho S P^2)^{1/3}.$$

Thus, in the ideal case ($\eta = 100\%$)

$$T_{ideal} = (2\rho S P^2)^{1/3}. \quad (10)$$

For a real propeller with efficiency $\eta < 1$ the thrust is reduced to

$$T_{exp} = \eta T_{ideal} = \eta (2\rho S P^2)^{1/3}. \quad (11)$$

Blade tip speed

The blade-tip speed at a rotational speed N_{rpm} is

$$V_{tip} = \pi D \frac{N_{rpm}}{60}, \quad (12)$$

where D is the propeller diameter. For $D = 254 \times 10^{-3} m$ and $N_{rpm} = 10000$,

$$V_{tip} = \pi (254 \times 10^{-3}) \frac{10000}{60} \approx 1.33 \times 10^2 m/s \approx 133 m/s. \quad (13)$$

4 Simulation Analysis Setup

4.1 Boundary Conditions and Rotating Domain Setup

In the setup we have defined 2 domains .We have a rotating domain and a static domain. The rotating domain is the domain where the blades are rotating .while the static domain is domain that contain this rotating domain and generally it has a surrounding fluid environment around it .

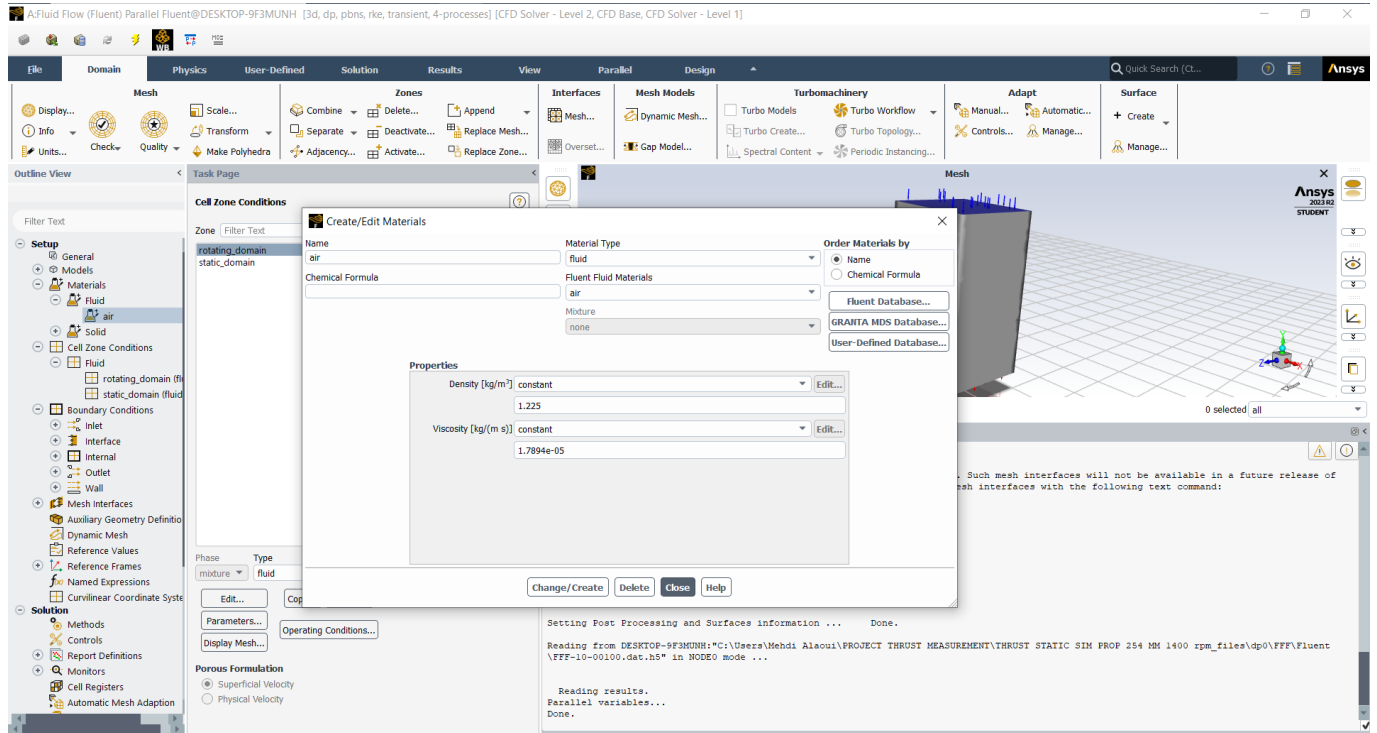


Figure 1: Definition of air material properties in ANSYS Fluent.

4.2 Inlet Boundary Condition

To represent a mildly distributed upstream conditions we prescribe the turbulence using the intensity-viscosity ratio method of 5 % and a turbulent viscosity ratio of 10. At the inlet, we impose a velocity boundary condition. The flow at the inlet is specified as a uniform velocity that is normal to the boundary in the frame.

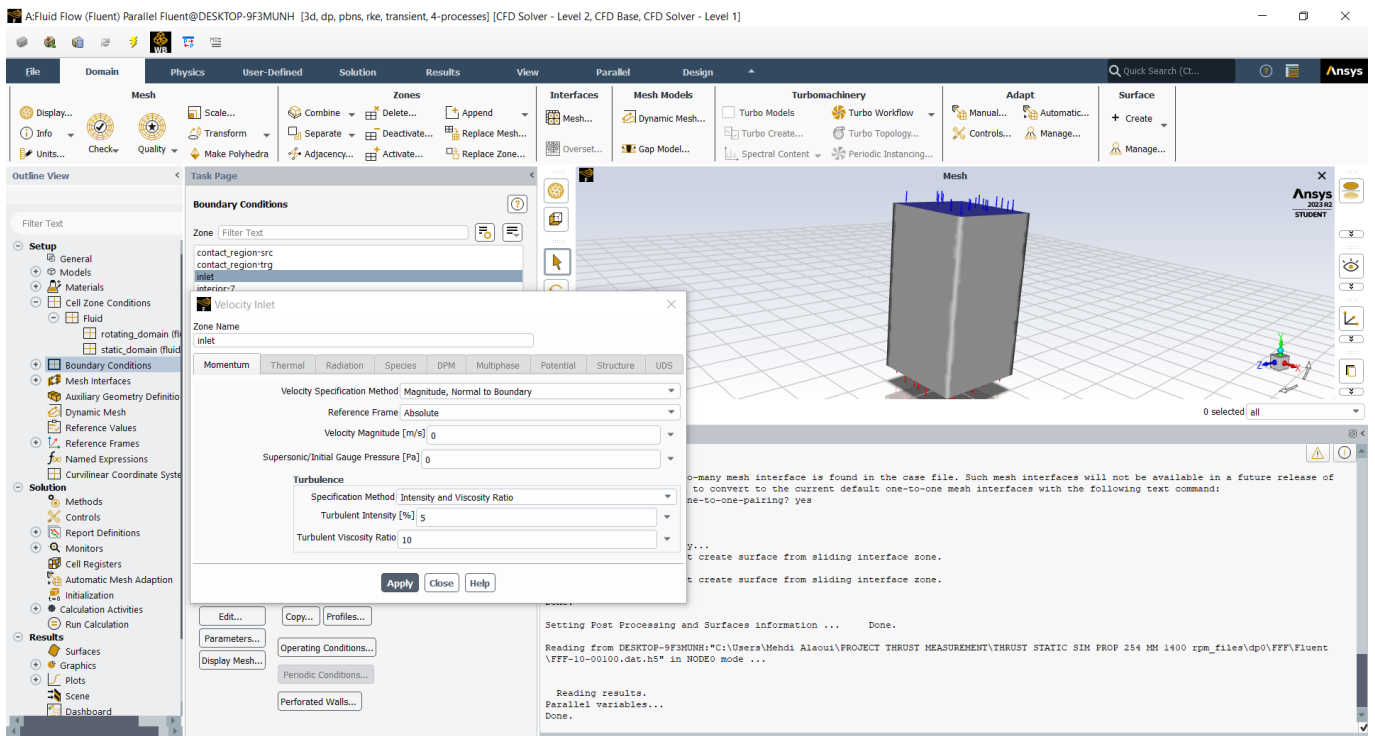


Figure 2: Velocity inlet boundary condition used in the CFD simulation.

4.3 Rotating Fluid Zone and Mesh Motion

In order to model the propeller, an inner rotating fluid zone around the blades was established by the configuration of the Fluent Workbench. Mesh motion has been activated for this zone, with a rotational speed of 1400 rpm prescribed about the propeller axis, while the surrounding outer domain remained stationary. No translational motion was imposed and the rotation axis origin was positioned at the propeller hub, aligned with the global shaft direction.

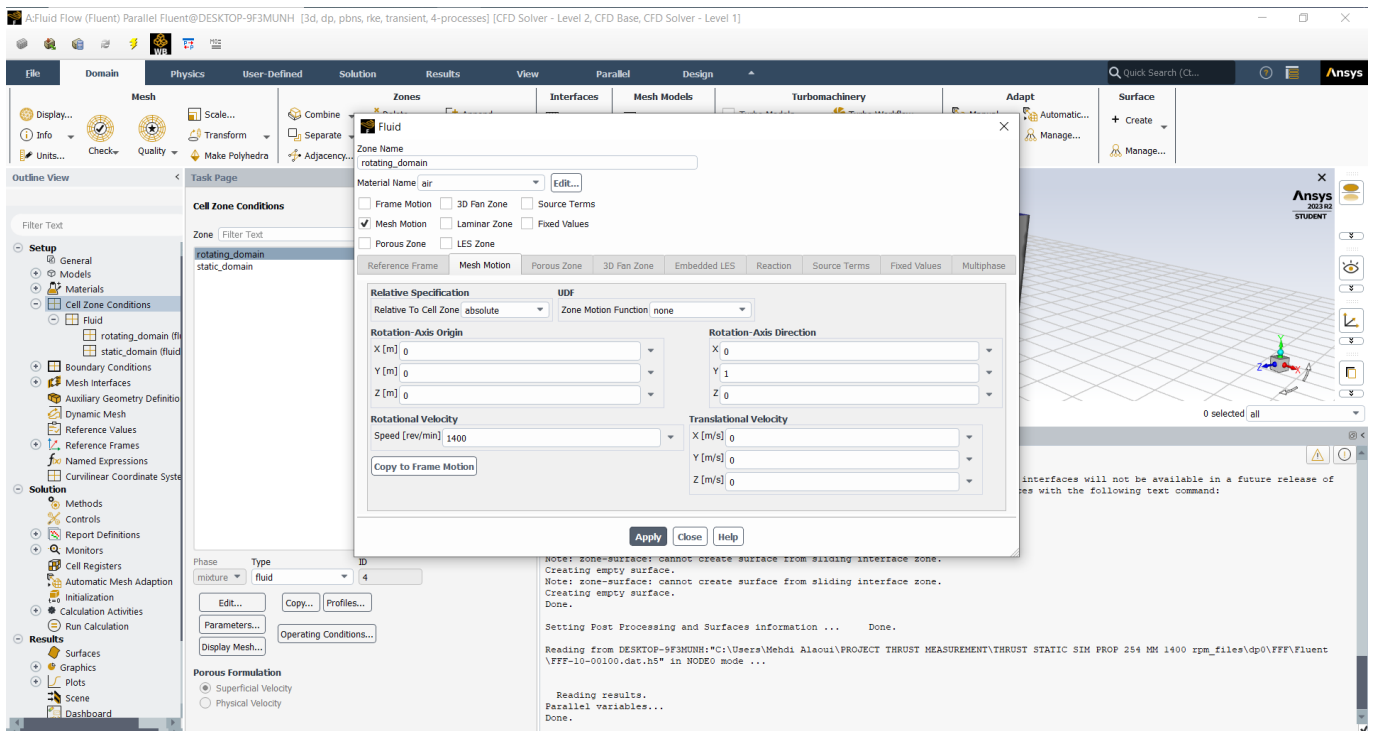


Figure 3: Rotational mesh motion specified for the rotating fluid domain.

4.4 Transient Solver and Time-Stepping Parameters

The transient simulation was advanced in time using a fixed time step. A user-specified time step size of 1.5×10^{-4} s was adopted, with 100 time steps and a maximum of 15 iterations per time step. This corresponds to a total physical simulation time of 0.015 s.

With the small time step, the unsteady flow caused by the rotating propeller is well resolved and the iteration limit is sufficient to reach convergence at each time step. Solution statistics and force reports were recorded at every time step in order to track the evolution of thrust over the course of the simulation.

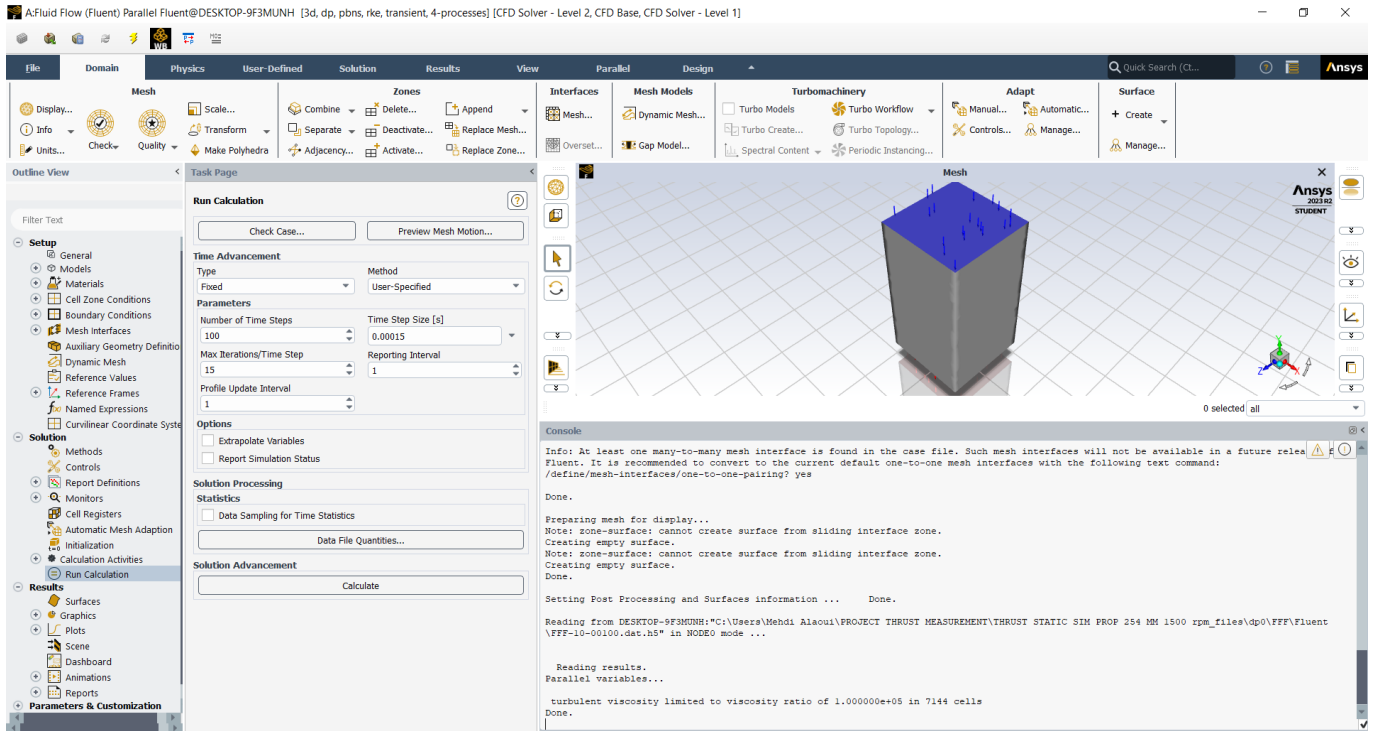


Figure 4: Transient run calculation settings used for the CFD simulation.

4.5 Computational Domain

The computational domain was designed in ANSYS Fluent Meshing as a rectangular enclosure surrounding the propeller, with a cylindrical rotating sub-domain embedded at the centre. The outer area, labelled Static Domain, describes the stationary far-field fluid volume; the inner Rotating Domain corresponds to the swept volume which the propeller is acting upon. The two regions are both defined as fluid, and this decomposition allows the propeller motion to be added by rotating only the inner domain while the outer enclosure is left fixed.

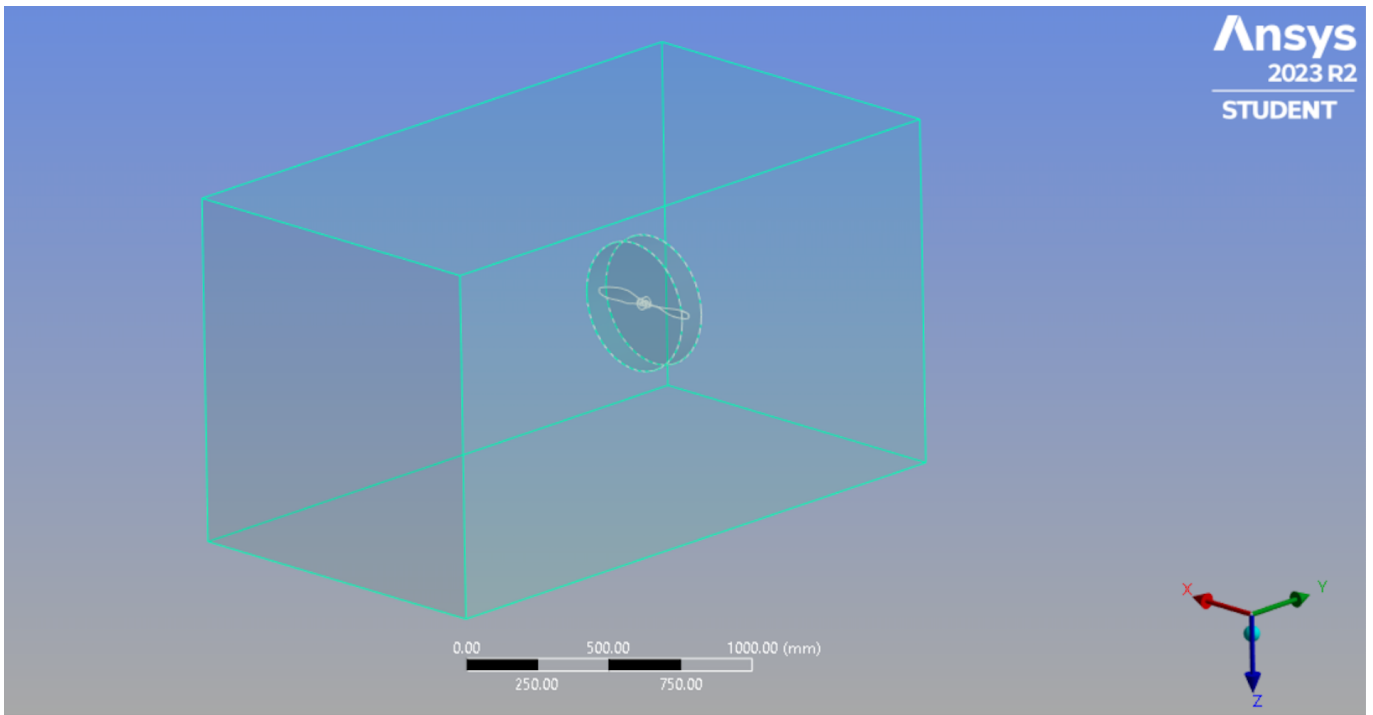


Figure 5: Computational domain in ANSYS Fluent Meshing showing the rotating and static fluid regions.

4.6 Local Mesh Refinement and Face Sizing

Local face sizing control on the rotating-disk region was performed to increase the mesh resolution near the propeller. The sizing is defined on 17 selected faces with a uniform element size of 40.0 mm. Curvature capture is enabled, using the default curvature normal angle of 18° and a growth rate of 1.2 so that the elements transition smoothly from the refined region to the coarser background mesh. This local refinement helps to resolve the pr

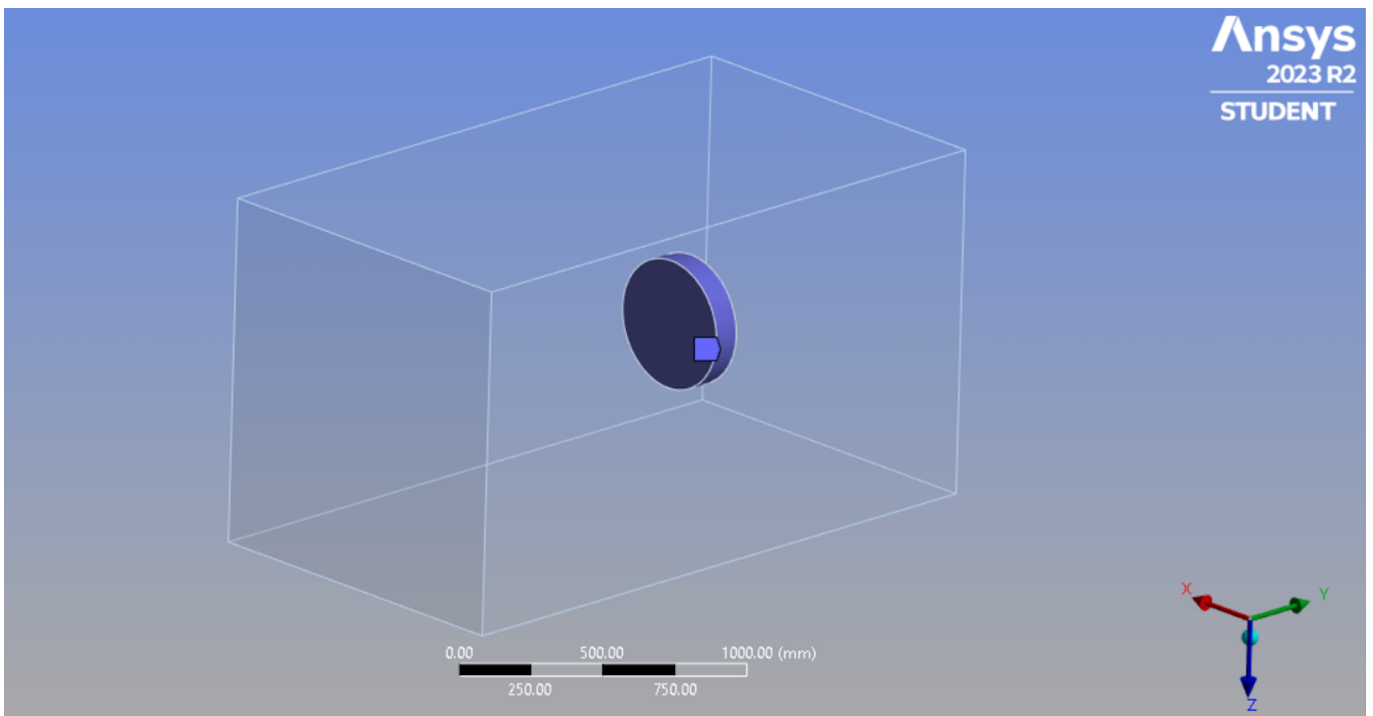


Figure 6: Location of the locally refined region using a face sizing control around the rotating disk.

Details of "Face Sizing" - Sizing	
Scope	
Scoping Method	Geometry Selection
Geometry	17 Faces
Definition	
Suppressed	No
Type	Element Size
<input type="checkbox"/> Element Size	40.0 mm
Advanced	
<input type="checkbox"/> Defeature Size	Default (0.4 mm)
Influence Volume	No
<input type="checkbox"/> Growth Rate	Default (1.2)
Capture Curvature	Yes
<input type="checkbox"/> Curvature Normal Angle	Default (18.0°)
<input type="checkbox"/> Local Min Size	Default (0.8 mm)
Capture Proximity	No

Figure 7: Face sizing parameters applied to the rotating region (element size 40.0 mm with curvature capture).

5 Meshing Parameters

- **Mesh Structure:** The meshing is applied to a cuboidal domain, with a clearly visible structured mesh comprising tetrahedral elements.

The element size is set to 80.0 mm, providing a relatively coarse mesh. Depending on the precision needed for the simulation results, this size may need adjustment.

- **Meshing Parameters:** Physics Preference: CFD (Computational Fluid Dynamics), which is suitable for fluid flow simulations involving the propeller.
- **Element Order:** Linear, which typically requires fewer computational resources compared to higher-order elements but may need refinement for capturing complex flow phenomena accurately.
- **Sizing and Defeaturing:**
 - Adaptive Sizing:** Disabled, indicating that a uniform mesh size is used throughout the domain.
- **Growth Rate:** Set to the default value (1.2), controlling how quickly the mesh size changes between adjacent cells.
- **Max Size:** 80.0 mm, consistent with the element size, ensuring uniformity.
- **Mesh Defeaturing:** Enabled with a default size of 0.4 mm, which helps in simplifying small geometric features that may not significantly impact the simulation results but could increase computational cost.

5.1 Global Mesh Generation and Discretisation

The non structured tetrahedral mesh was used to discretise the full computational domain. The background mesh had a global element size of 80.0 mm, and the curvature-based refinement was turned on. Adaptive sizing was disabled, while the default growth rate of 1.2 was maintained, enabling for a smooth transition from the locally refined region near the propeller to the coarser cells in far field regions. This mesh resolution ensures a reasonable balance between solution accuracy and computational cost for the current simulations.

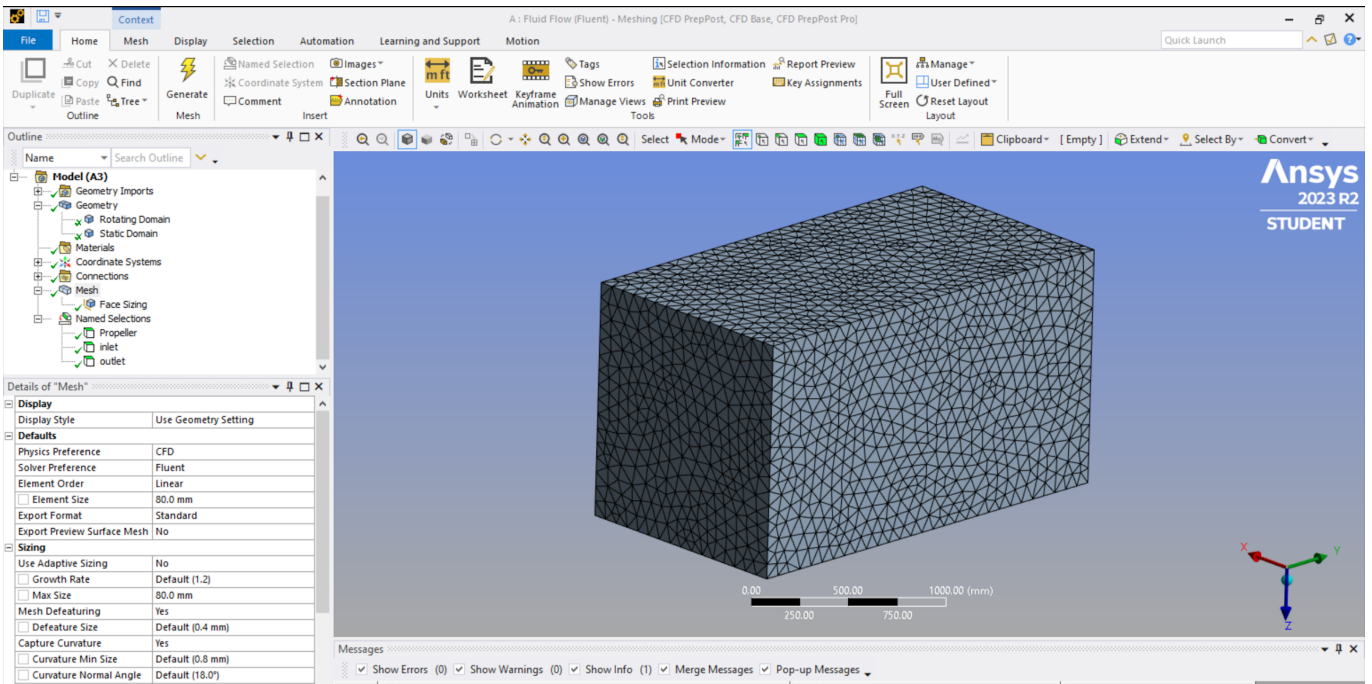


Figure 8: Unstructured tetrahedral mesh of the computational domain in ANSYS Fluent Meshing.

5.2 Propeller Geometry and Named Selection

ANSYS Fluent Meshing and a dedicated named selection Propeller was developed for all blade and hub faces. It consists of 14 faces with a total surface area of 38 006 mm², as reported in the details panel. Turn on the Send to Solver option so that the same set of faces can be found in Fluent, while the surface is kept visible. Program-controlled inflation is eliminated in favor of manual control of the near-wall mesh if required. Defining the propeller as indicated in this way ensures that thrust and other aerodynamic loads can be consistently evaluated by adding the pressure and viscous forces over exactly the same surfaces in each simulation.

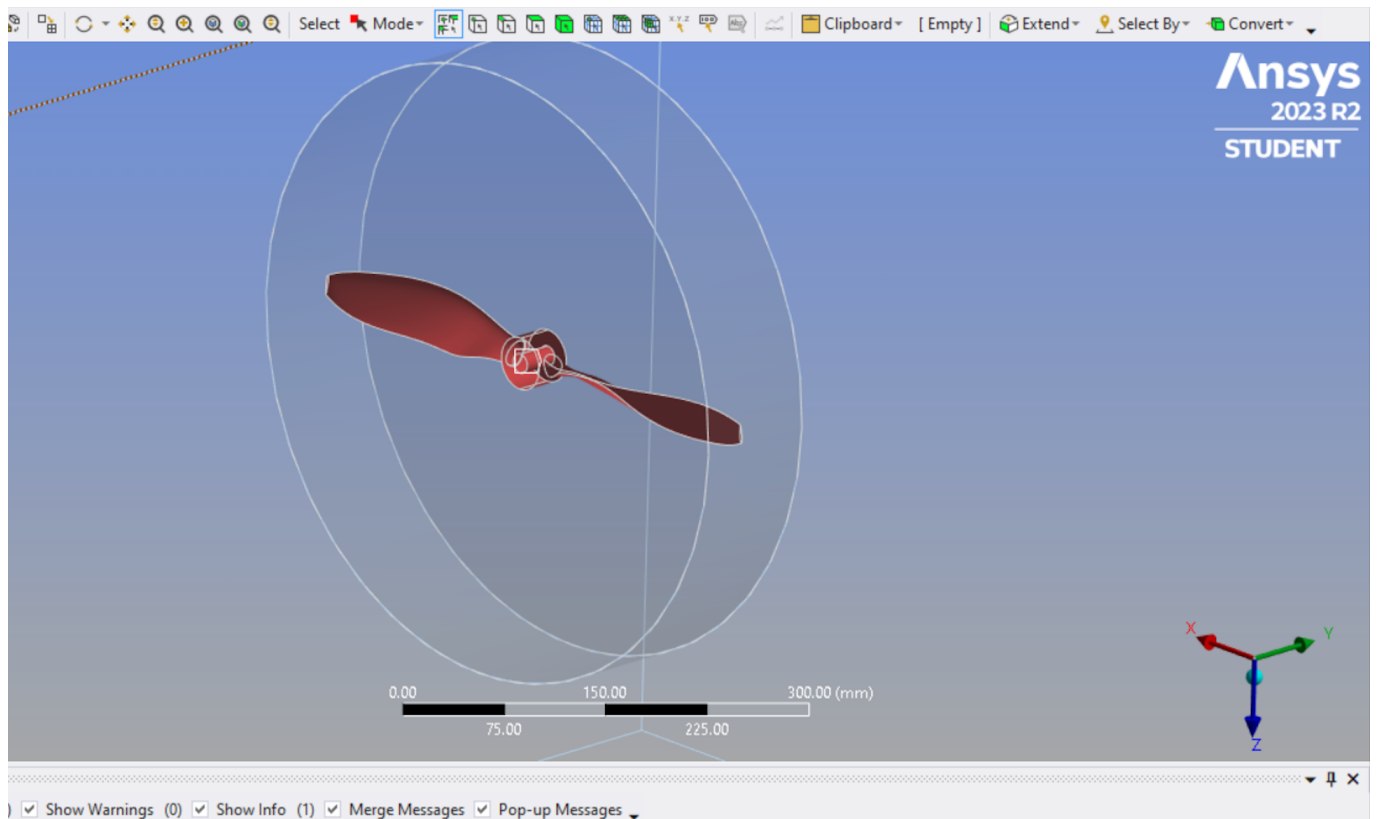


Figure 9: Named selection of the propeller surface in ANSYS Fluent Meshing.

Details of "Propeller"	
Scope	
Scoping Method	Geometry Selection
Geometry	14 Faces
Definition	
Send to Solver	Yes
Protected	Program Controlled
Visible	Yes
Program Controlled Inflation	Exclude
Statistics	
Type	Manual
<input type="checkbox"/> Total Selection	14 Faces
<input type="checkbox"/> Surface Area	38006 mm ²
Suppressed	0
Used by Mesh Worksheet	No

Figure 10: Details of the *Propeller* named selection, including face count and surface area.

5.3 Thrust Force Post Processing

The thrust generated by the propeller was extracted using a surface force report defined in ANSYS Fluent. A new report named thrust-force was created in the Report Definitions panel, with the zone list restricted to the propeller surface only. The force vector was defined in the axial direction so that the resulting integral corresponds to the propulsive thrust component. The result was written to a report file and a report plot with a sampling frequency of one time step, allowing the time evolution of thrust to be monitored over the entire transient simulation. This post-processing setup ensures that the thrust values calculated for comparison with the theoretical model and for performance assessment are obtained consistently from the CFD solution.

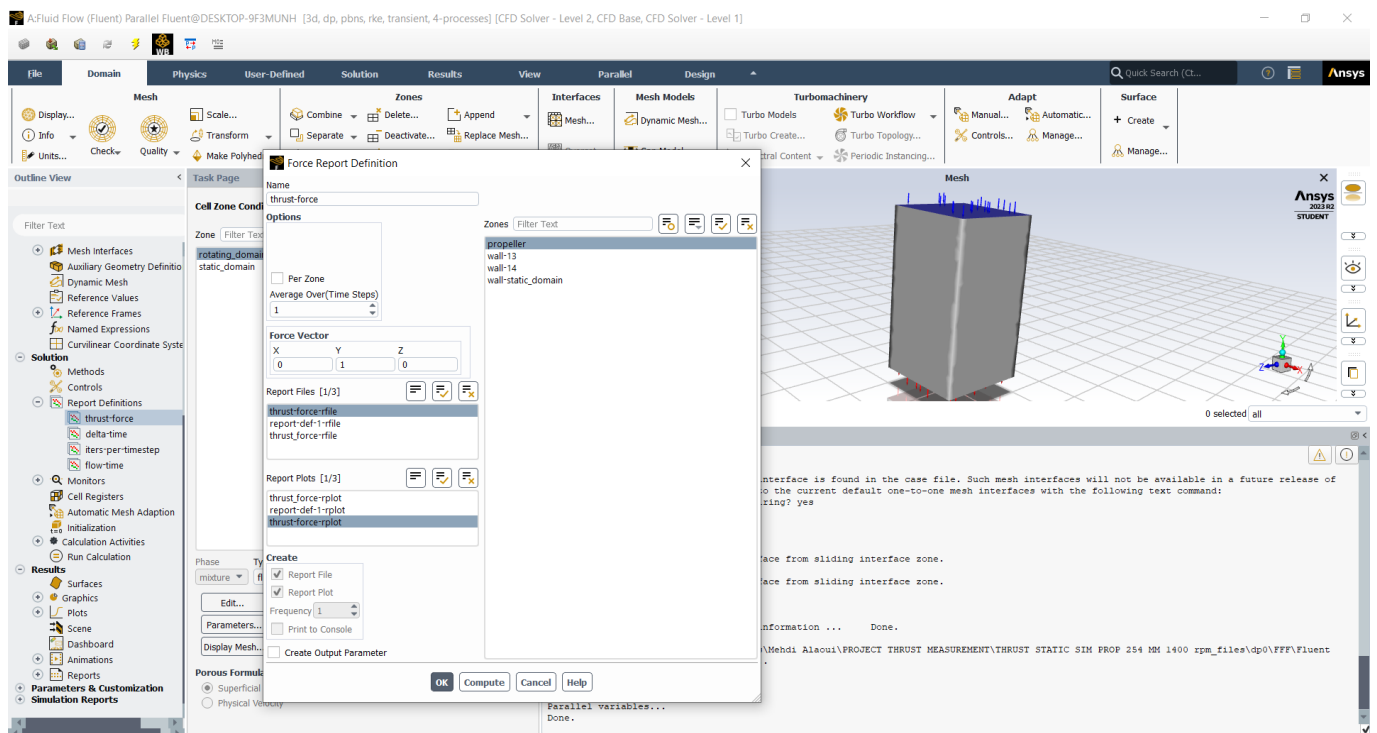


Figure 11: Force report definition used to record the propeller thrust in ANSYS Fluent.

6 Simulation Results

Figure 12 shows the velocity magnitude contours on a longitudinal cut through the propeller. The flow flows fast over the suction side of the blade and forms a high-velocity region which flows downstream to slipstream, where lower speeds are observed in quiescent fluid surrounding it. For the majority of the span, the wake stays attached to the blade, as velocity continues to decay with a jet mixing with the ambient flow. The contour plot substantiates that the propeller is capable of producing a coherent axial jet and that the predominant thrust contribution is correlated with strong acceleration occurring around the blade surfaces.

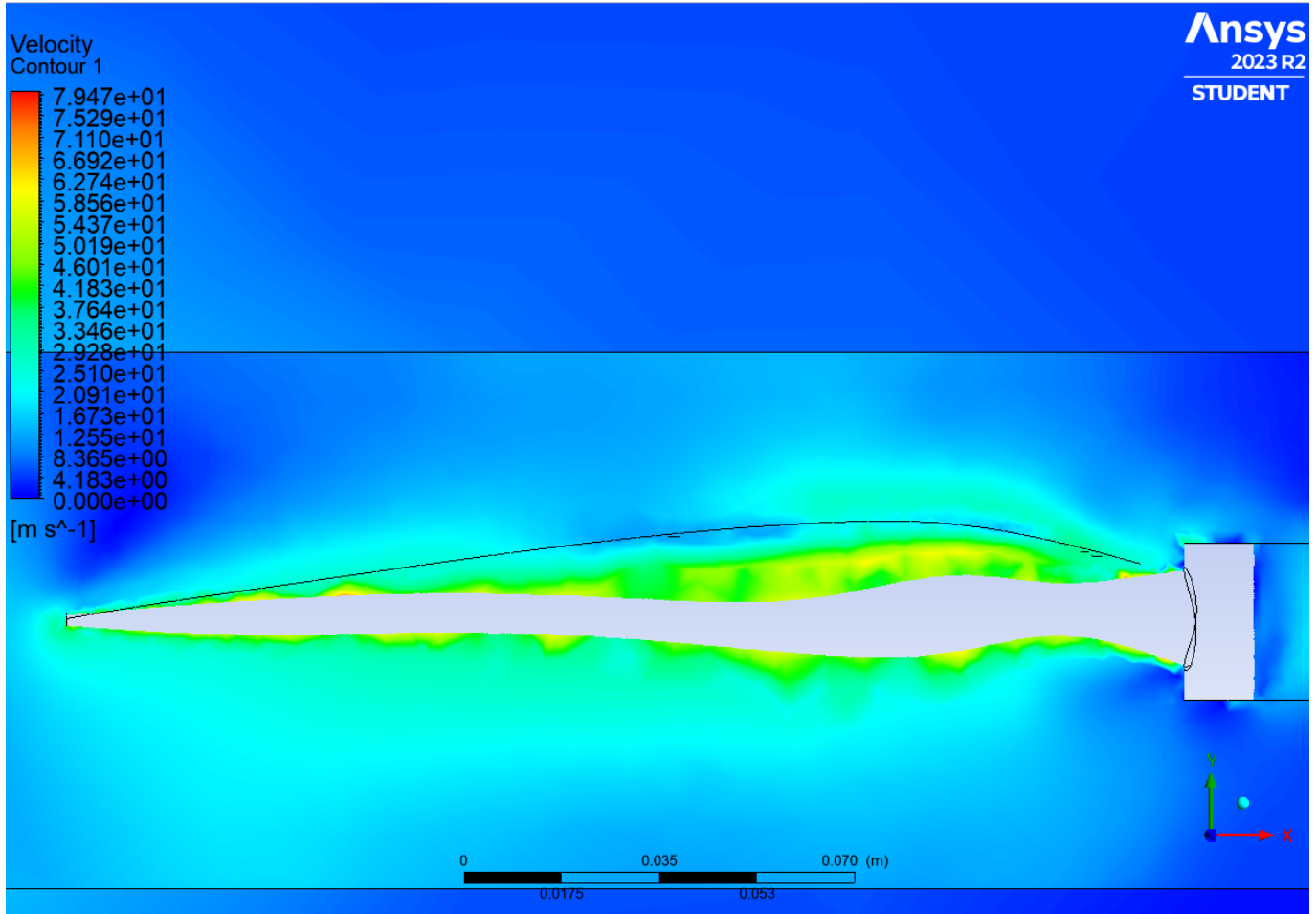


Figure 12: Velocity magnitude contours in a longitudinal plane through the propeller, showing the accelerated slipstream generated by the rotating blades.

6.1 Resulting Thrust Force at Different Rotational Speeds

The thrust generated by the propeller was obtained from a surface force report acting on the propeller wall zone, with the direction vector aligned with the axial (y) direction. For each rotational speed, Fluent reports the net pressure and viscous contributions and their sum, which is used as the CFD estimate of the static thrust.

At the lowest speed of 1400 rpm, the integrated axial force on the propeller is approximately $T \approx 4.39 \text{ N}$. The load is dominated by the pressure contribution, while viscous shear plays a minor role.

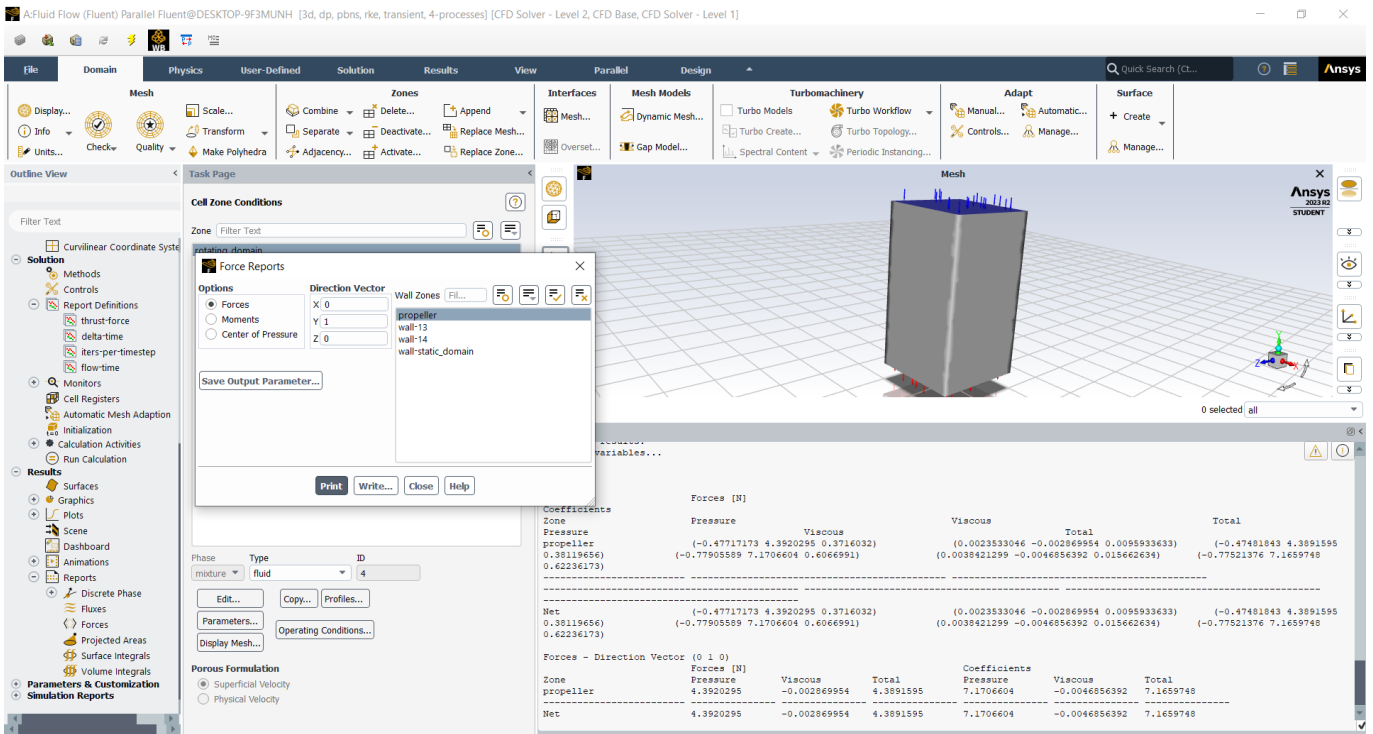


Figure 13: Resulting thrust force at 1400 rpm obtained from the Fluent surface force report on the propeller.

Increasing the speed to 1500 rpm leads to a thrust of about $T \approx 10.1 \text{ N}$ (Figure 14), more than double the 1400 rpm value, consistent with the expected quadratic dependence of thrust on rotational speed for a propeller operating in static conditions.

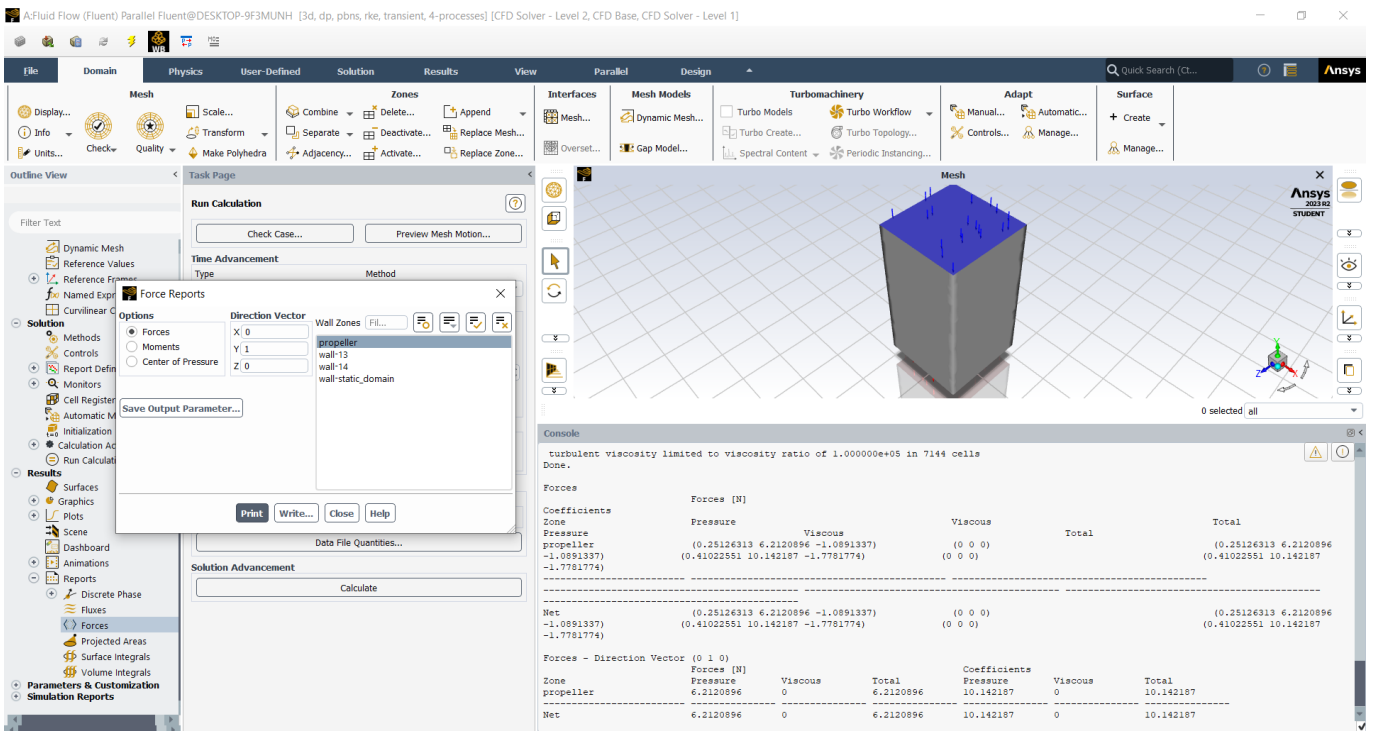


Figure 14: Resulting thrust force at 1500 rpm. The reported total axial force is approximately 10.1 N.

At the highest simulated speed of 2000 rpm, the computed thrust reaches approximately $T \approx 16.9 \text{ N}$, as shown in Figure 15. The monotonic increase of thrust with ω and the approximate $T \propto \omega^2$ trend are in line with the simple theoretical analysis presented earlier.

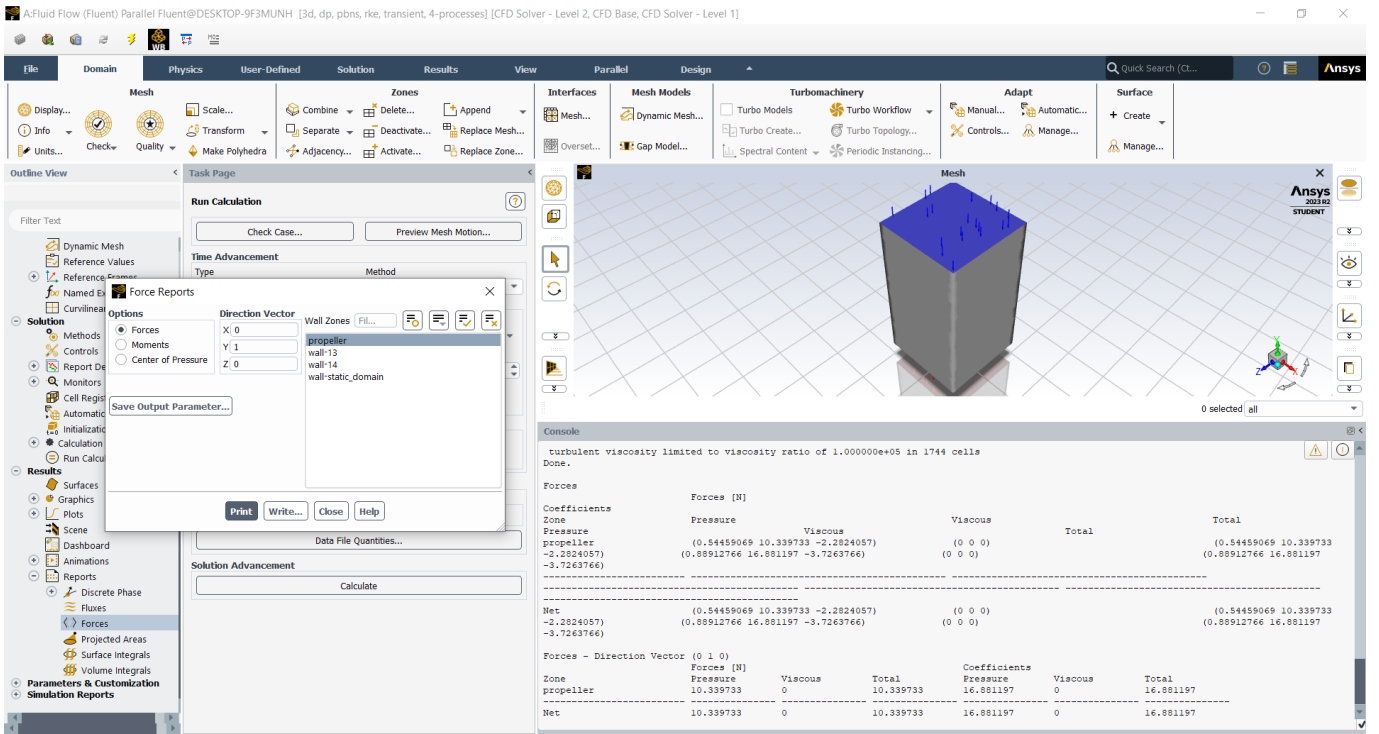


Figure 15: Resulting thrust force at 2000 rpm from the Fluent force report; the net axial force on the propeller is about 16.9 N.

7 Transient Thrust Response

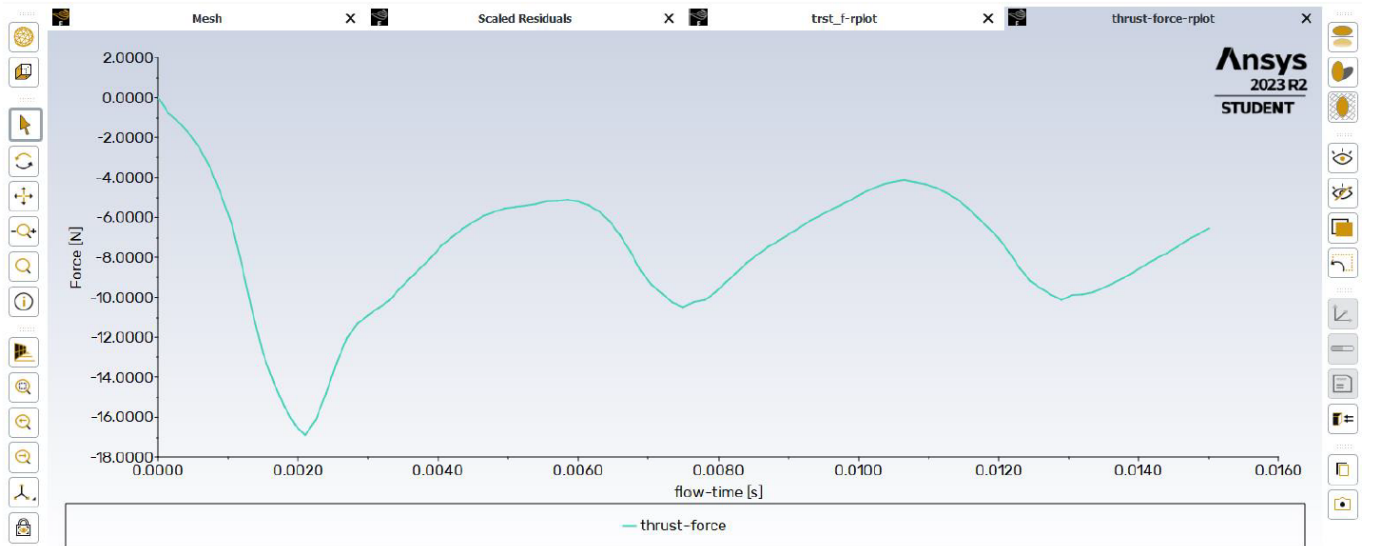


Figure 16: Time history of the propeller thrust force during the transient simulation.

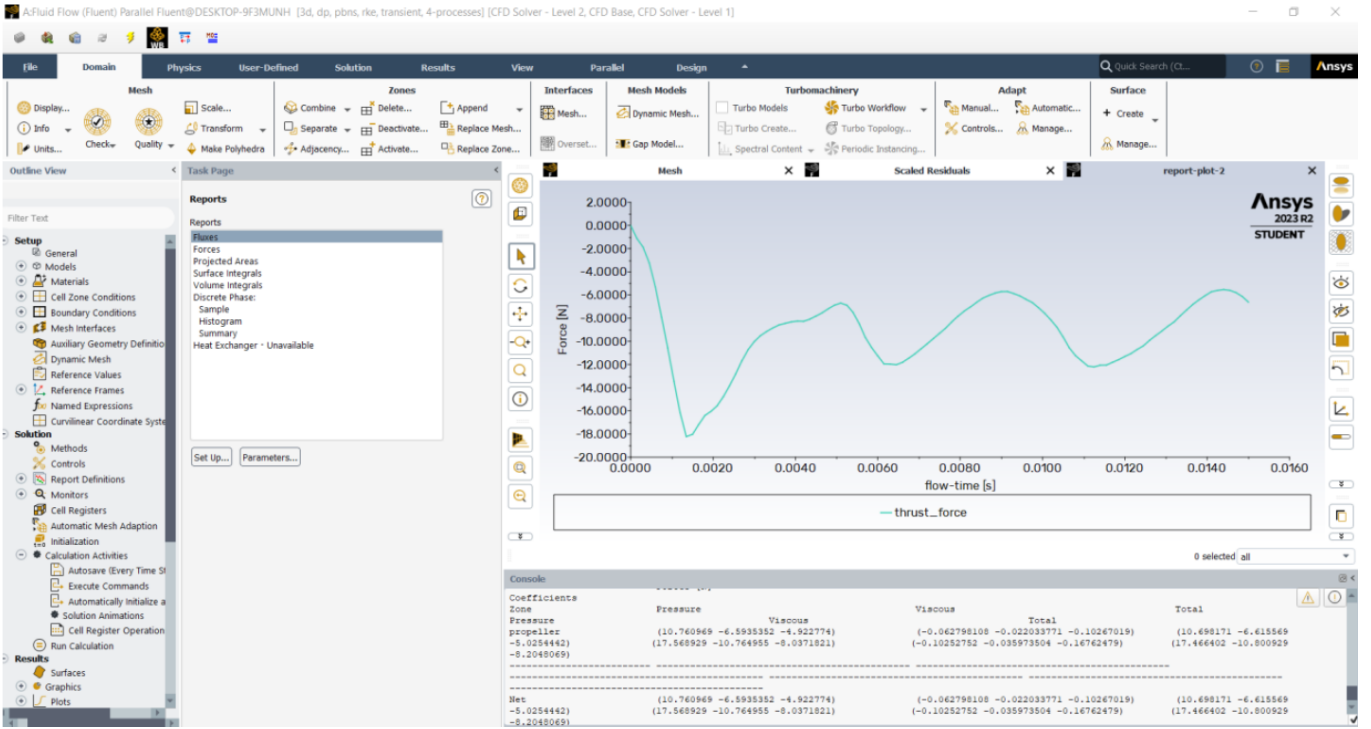


Figure 17: Fluent thrust-force report plot used to evaluate convergence and mean thrust.

Table 1: CFD-predicted static thrust for the 254 mm propeller at different rotational speeds.

Rotational speed Ω (rpm)	Axial thrust T (N)
1400	4.39
1500	10.1
2000	16.9

8 Conclusion

In this Project, we presented a 3D transient CFD simulation of the static thrust of a 254 mm airfoil-based propeller in ANSYS Fluent. The propeller motion was described by an inner rotating fluid zone, which is placed in a stationary outer domain (discretized by an unstructured tetrahedral mesh), which was then characterized by the realizable k-epsilon turbulence model. According to the surface force reports results, the predicted thrust on the propeller is calculated to be 4.39 N at 1400 rpm, 10.1 N at 1500 rpm, and 16.9 N at 2000 rpm. This monotonic increase seems to fit within the framework of the quadratic relationship between thrust and rotational speed, aligning well with the simplified theoretical view. The magnitude of velocity contours establishes a physically relevant accelerated slipstream and high-velocity areas on the suction side of the blades in consideration of the forces proposed based on rough estimates. On the other hand, the mesh is coarse, and the operating points in this approach are limited, and it could be said that the results are more representative than convergent, (because of the computational limits of our machines, it is hard to achieve convergence with our setups, but results are satisfying and coherent). Future work shall include the refinement of the mesh, a larger set of rotational speeds, and comparison with some stand tests to be able to validate and calibrate the CFD model.

8.1 Computational Resources

The simulations were carried out on workstations equipped with Intel Core i7 and AMD Ryzen 5 processors, NVIDIA GTX 350 and RTX 3060 GPUs.